Inorganic Chemistry

Article

pubs.acs.org/IC

Polyclusters and Substitution Effects in the Na–Au–Ga System: Remarkable Sodium Bonding Characteristics in Polar Intermetallics

Volodymyr Smetana, Gordon J. Miller, and John D. Corbett*

Ames Laboratory-DOE and Department of Chemistry, Iowa State University, Ames, Iowa 50011, United States

Supporting Information

ABSTRACT: A systematic exploration of Na- and Au-poor parts of the Na–Au–Ga system (less than 15 at. % Na or Au) uncovered several compounds with novel structural features that are unusual for the rest of the system. Four ternary compounds $Na_{1.00(3)}Au_{0.18}Ga_{1.82(1)}$ (**I**), $NaAu_2Ga_4$ (**II**), $Na_5Au_{10}Ga_{16}$ (**III**), and $NaAu_4Ga_2$ (**IV**) have been synthesized and structurally characterized by single crystal X-ray diffraction: $Na_{1.00(3)}Au_{0.18}Ga_{1.82(1)}$(**I**, *P6/mmm*, a = 15.181(2), c =9.129(2)Å, Z = 30); $NaAu_2Ga_4$ (**II**, *Pnma*, a = 16.733(3), b = 4.3330(9), c =7.358(3) Å, Z = 4); $Na_5Au_{10}Ga_{16}$ (**III**, $P6_3/m$, a = 10.754(2), c =11.457(2) Å, Z = 2); and $NaAu_4Ga_2$ (**IV**, $P2_1/c$, a = 8.292(2), b = 7.361(1), c =9.220(2)Å, β = 116.15(3), Z = 4). Compound **I** lies between the large family of Bergman-related compounds and Na-poor Zintl-type compounds and exhibits a clathrate-like structure containing icosahedral clusters similar to those in cubic 1/1 approximants, as well as tunnels with highly disordered cation positions and fused Na-centered clusters. Structures **II**, **III**, and **IV** are built of polyanionic networks and clusters that generate novel tunnels in each that contain isolated, ordered Na atoms. Tight-binding electronic structure calculations using linear muffin-tin-orbital (LMTO) methods on **II**, **III**, **IV** and an idealized model of **I** show that all are metallic with evident pseudogaps at the Fermi levels. The integrated crystal orbital Hamilton populations for **II**–**IV** are typically dominated by Au–Ga, Ga–Ga, and Au–Au bonding, although Na–Au and Na–Ga contributions are also significant. Sodium's involvement into such covalency is consistent with that recently reported in Na–Au–M (M = Ga, Ge, Sn, Zn, and Cd) phases.

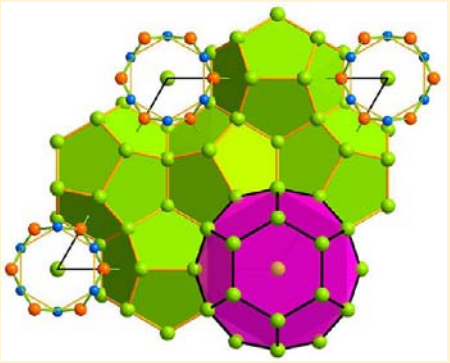

INTRODUCTION

Systems involving an alkali or alkaline-earth metal, gold, and a post-transition element such as Ga or In have fruitfully yielded numerous new intermetallic compounds with some unprecedented structural and bonding features.[1] They include polyanionic or polycationic networks of tunnels with ordered or disordered cations,[2,3] isolated Au_n-clusters,[4] 2- or 3-D Au frameworks[5,6] and the unusual participation of an alkali metal in covalent bonding.[7] Strong polar-covalent bonding between Au and post-transition elements enhances formation of heteroatomic, polyanionic clusters and nets,[2,8] whereas homoatomic conglomerates become more evident on increasing Au content.[4] The structural behavior of alkali metals also depends on their concentration, as well as cation/anion size ratios. For example, compounds with 10–20 atomic % alkali metal have the metal completely encapsulated by the polyanionic framework. Here, the alkali metal certainly stabilizes the structure while exhibiting very limited participation in covalent bonding. On the other hand, large cations such as Cs and Rb in low proportions, e.g., in $RbGa_7$ and $CsGa_7$, may form polycationic networks with encapsulated anions or anionic clusters.[9,10] Of course, the electropositive elements cannot be considered independent components because both polyanionic and polycationic constituents interpenetrate and form similar motifs. Cardinally different situations are observed for 20–35 at. % active metal, especially concerning Na's participation in covalent bonding. Perhaps the best examples of this are the Bergman-type Na–Au–Ga phases.[11] Their crystal structures represent a packing of clusters with local fivefold symmetry that contain an icosahedron at the center. This family does not yet include any heavier alkali metal representatives. The reduced likelihood of such icosahedral-based structures for the heavier alkali metals may arise from large differences in both electronegativities and atomic sizes between the alkali metal and Au, Ga, In, leading to higher coordination numbers. Of course, we should also mention Bergman phases with Li,[12−15] but, in general, this element behaves very differently than the other alkali metals by playing combined roles in polar intermetallics.[15] Na, with its relatively small size, is still considerably larger than Li and is insufficiently electronegative to become a part of a polyanionic net as Li does. Nonetheless, Na turns out to be an ideal alkali metal with which to form novel polar intermetallic compounds.[3,8,16,17]

Recent investigations of the Na–Au–Ga system have uncovered several new compounds in the ∼15–33 at. % Na concentration range, including a new quasicrystal. All these compounds can be characterized as valence electron poor, polar intermetallics that are situated between Zintl and Hume–Rothery phases. They are metallic conductors, although polar–

Received: June 21, 2013
Published: October 18, 2013

   dx.doi.org/10.1021/ic401580y | *Inorg. Chem.* 2013, 52, 12502–12510

Table 1. Details of the Crystal Structure Investigations and Refinement

Empirical formula/Z	$NaAu_{0.18}Ga_{1.82(1)}$(**I**)/30	$NaAu_2Ga_4$(**II**)/4	$Na_5Au_{10}Ga_{16}$(**III**)/2	$NaAu_4Ga_2$(**IV**)/4
Formula weight	185.3	695.8	3200.14	950.3
Temperature, K		293		
Wavelength, Å		0.71073		
Crystal system	hexagonal	orthorhombic	hexagonal	monoclinic
Space group	*P6/mmm*	*Pnma*	$P6_3/m$	$P2_1/c$
a, Å	15.181(2)	16.733(3)	10.754(2)	8.292(2)
b, Å	15.181(2)	4.3330(9)	10.754(2)	7.361(1)
c, Å	9.129(2)	7.358(3)	11.457(2)	9.220(2)
β	-	-	-	116.15(3)
Volume, Å^3	1822.0(5)	533.5(2)	1147.5(3)	505.2(2)
ρ (calculated), g/cm^3	5.066	8.663	9.262	12.494
μ, mm^{-1}	30.738	74.616	82.125	126.139
F(000)	2449	1172	2682	1556
θ range	1.55° to 28.52°	3.02° to 26.74°	2.19° to 26.7°	2.74° to 27.58°
Index ranges	$-19 \le h \le 19$	$-21 \le h \le 21$	$-13 \le h \le 11$	$-10 \le h \le 10$
	$-19 \le k \le 19$	$-7 \le k \le 7$	$-13 \le k \le 12$	$-9 \le k \le 9$
	$-12 \le l \le 12$	$-9 \le l \le 9$	$-13 \le l \le 14$	$-11 \le l \le 11$
Refinement method		Full-matrix least-squares on F^2		
Data/restraints/parameters	949/0/57	564/0/44	807/0/53	1167/0/60
Goodness-of-fit on F^2	1.14	1.06	1.02	1.03
Final *R* indices $[I > 2\sigma(I)]^a$	R_1 = 0.049, wR^2 = 0.103	R_1 = 0.057, wR^2 = 0.074	R_1 = 0.033, wR^2 = 0.055	R_1 = 0.028, wR^2 = 0.058
R indices (all data)	R_1 = 0.070, wR^2 = 0.113	R_1 = 0.109, wR^2 = 0.082	R_1 = 0.053, wR^2 = 0.059	R_1 = 0.037, wR^2 = 0.061
R_{int}	0.095	0.079	0.097	0.062
Larg. peak and hole, e$^-$/Å^3	3.356 and −1.759	2.526 and −2.902	3.088 and −3.065	3.441 and −3.074

covalent interactions play significant roles in their stability and features.[18,19] Additional combinations of Na, Au, and Ga or In have been especially unique toward forming numerous structures with local fivefold symmetry.[7,16,20−23] In these systems, Au appears to be an exceptional oxidizing agent and mixes with the triels, due to its large electronegativity and small size arising from relativistic effects.[24] However, Au also lowers valence electron concentrations. These features are illustrated by compounds on the line of ∼33 at. % Na between the two binaries, Na_7Ga_{13},[21] and $NaAu_2$.[25] Eight compounds, including two with ∼15 at. % Na content, have been characterized. They all exhibit clusters with local 2D or 3D fivefold symmetry including the newly observed $Na_{13}Au_{12}Ga_{15}$ *i*-QC.[7] The Na-rich structures contain mixed Au/Ga position(s), whereas the Na-poor compounds $Na_{0.56}Au_2Ga_2$ and $Na_{13}Au_{41.2}Ga_{30.3}$[3] show full separation of Au and Ga into tunnel structures and Na atom encapsulation by the polyanionic network.[3] These structural chemical differences have increased our interest in the rest of the Na−Au−Ga system, especially in the unexplored Ga-rich section, to provide a more complete picture of their structure−bonding relationships. In this work, we report four new compounds in the rest of the Na−Au−Ga system that represent new structure types and unusual structural motifs.

EXPERIMENTAL SECTION

Synthesis. Starting materials were Na ingots (99.95%, Alfa Aesar), with surfaces manually cleaned with a surgical blade, Au particles (99.999%, BASF) and Ga ingots (99.999%, Alfa Aesar). Reaction mixtures of 250−400 mg total were weighed in a N_2-filled glovebox (H_2O < 0.1 ppmv) and loaded into 9 mm Ta ampules that were sealed by arc welding under Ar. These ampules were subsequently enclosed in evacuated SiO_2 jackets. Temperature conditions were chosen according to Ga content: (i) Ga-rich samples were heated at 500 °C for 2−5 h, cooled to 350 °C at a rate of 5−10 °C/h, then annealed there for 6−10 days, and quenched into water; (ii) Au-rich samples were heated at 700 °C for only 2−3 h to prevent corrosion of the Ta tube, quenched into water, and then annealed at 350 °C for 7 days. Experimental and simulated powder patterns of ∼$Na_1Au_{0.18}Ga_{1.82}$, $Na_5Au_{10}Ga_{16}$, and $NaAu_4Ga_2$ can be found in Supporting Information (Figures S1, S2, and S3).

Single crystals of each of the four compounds could be obtained easily from several samples, even those containing very minor parts of a designated phase. Several samples around composition **I** were prepared to check the possibility of a homogeneity range that has been found in some related compounds;[26] however, no shifts of the unit cell parameters beyond acceptable 3σ limits were detected, and this compound appears to be a line composition. **II**−**IV** do not show any indication of Au/Ga mixing in contrast to **I**. Within the series, **I**−**III** have silvery metallic luster, and **IV** has a slightly yellow undertone because of the high Au content. **III** and **IV** are stable against long-time exposure to air or water at room temperature, whereas **I** and **II** show partial surface oxidation after 5−7 days. The high stability of **I** remains unusual in view of the full hydrolysis of the compositionally related $Na_{17}Au_{5.9}Ga_{46.6}$[20] within several days.

X-ray Diffraction Studies. Phase analyses were performed using powder diffraction data collected at 290 K with the aid of a STOE STADI P powder diffractometer equipped with an area detector and Cu $K_{\alpha 1}$ radiation (λ = 1.54059 Å). The samples were dispersed on Mylar sheets with the help of vacuum grease and fixed to the holder using split Al rings. The lattice parameters were refined using the WinXPow program.[27] The overall phase diagram for the Na−Au−Ga system around 350$^\sigma$ that has resulted according to our extended X-ray investigationsis summarized in Figure S4.

Single crystals were fixed on glass fibers. Single-crystal diffraction data were collected at room temperature on a Bruker SMART APEX CCD diffractometer with Mo K_α radiation in the form of three sets of 606 frames with 0.3° scans in ω and exposures of 10 s per frame. The reflection intensities were integrated with the SAINT program in the SMART software package[28] over the entire reciprocal sphere. Empirical absorption corrections were accomplished with the SADABS program.[29] Space groups were determined by XPREP algorithms within the SHELXTL97 program package,[30] which suggested space groups *P6/mmm*, *Pnma*, $P6_3/m$, and $P2_1/c$, respectively, for **I**−**IV**. The starting atomic parameters were obtained via direct methods and refined using the program SHELXTL-97 (full matrix least-squares on

dx.doi.org/10.1021/ic401580y | *Inorg. Chem.* 2013, 52, 12502−12510

Table 2. Atomic Coordinates and Equivalent Thermal Displacement Parameters for $NaAu_{0.2}Ga_{1.8}$ (I)

Atom	Site	x	y	z	U_{eq}	SOF
Au1/Ga1	6*m*	0.2084(1)	0.60420(7)	1/2	0.0187(6)	0.240/0.760(8)
Au2/Ga2	12*n*	0	0.2099(1)	0.2828(1)	0.0369(5)	0.327/0.673(6)
Ga3	12*p*	0.1629(1)	0.4948(1)	0	0.0119(4)	1
Ga4	12*n*	0	0.3558(1)	0.1496(2)	0.0130(4)	1
Ga5	12*o*	0.1031(1)	0.55157(6)	0.2542(2)	0.0122(4)	1
Ga6	6*m*	0.8888(1)	0.1112(1)	1/2	0.0223(6)	1
Na1	4*h*	1/3	2/3	0.2000(1)	0.032(3)	1
Na2	12*o*	0.2115(3)	0.7885(3)	0.3067(1)	0.037(2)	1
Na3	6*k*	0	0.3782(8)	1/2	0.040(3)	1
Na4	6*l*	0.1342(5)	0.2684(9)	0	0.049(3)	1
Na5	2*e*	0	0	0.2642(5)	0.26(10)	0.65(16)
Na6	2*e*	0	0	0.3774(5)	0.26(10)	0.27(9)
Na7	2*e*	0	0	0.1424(5)	0.26(10)	0.13(10)

F^2), uiltimately with anisotropic atomic displacement parameters for all atoms. Details of data collection and refinement are presented in Table 1, and the atomic positions and equivalent displacement parameters are listed in Tables 2 and 3. The anisotropic parameters of all independent atoms and additional crystallographic information are provided in Supporting Information in the form of cif files.

Table 3. Atomic Coordinates and Equivalent Thermal Displacement Parameters for II, III, and IV

Atom	Site	x	y	z	U_{eq}
		$NaAu_2Ga_4$ (II)			
Au1	4*c*	0.4770(1)	1/4	0.7588(4)	0.0169(7)
Au2	4*c*	0.2192(1)	1/4	0.5016(4)	0.0212(7)
Ga1	4*c*	0.3156(3)	1/4	0.8054(9)	0.013(2)
Ga2	4*c*	0.4358(3)	3/4	0.9440(9)	0.018(2)
Ga3	4*c*	0.4521(3)	3/4	0.5574(9)	0.015(2)
Ga4	4*c*	0.3009(3)	3/4	0.5729(9)	0.018(2)
Na1	4*c*	0.376(1)	1/4	0.256(4)	0.031(6)
		$Na_5Au_{10}Ga_{16}$ (III)			
Au1	2*b*	0	0	0	0.0105(3)
Au2	6*h*	0.40255(8)	0.26417(8)	1/4	0.0092(2)
Au3	12*i*	0.45790(6)	0.29700(6)	0.89106(5)	0.0145(1)
Ga1	12*i*	0.3854(2)	0.4219(2)	0.0798(1)	0.0110(4)
Ga2	6*h*	0.6006(2)	0.5447(2)	1/4	0.0118(5)
Ga3	12*i*	0.2783(2)	0.1256(2)	0.0564(1)	0.0125(4)
Ga4	2*c*	2/3	1/3	3/4	0.021(1)
Na1	4*f*	2/3	1/3	0.0892(8)	0.017(2)
Na2	6*h*	0.1019(9)	0.2023(8)	1/4	0.019(2)
		$NaAu_4Ga_2$ (IV)			
Au1	4*e*	0.82322(7)	0.10332(8)	0.65587(7)	0.0074(2)
Au2	4*e*	0.14499(7)	0.21589(8)	0.92129(7)	0.0053(2)
Au3	4*e*	0.63365(8)	0.39607(8)	0.45333(7)	0.0118(2)
Au4	4*e*	0.62911(8)	0.84580(8)	0.73400(7)	0.0077(2)
Ga1	4*e*	0.4833(2)	0.1754(2)	0.5850(2)	0.0079(4)
Ga2	4*e*	0.0033(2)	0.8686(2)	0.8877(2)	0.0057(3)
Na1	4*e*	0.7890(8)	0.0449(9)	0.3248(8)	0.013(1)

Electronic Structure Calculations. Calculations for II–IV and hypothetical "$Na_{30}Au_6Ga_{54}$" for I were performed by means of the self-consistent, tight-binding, linear-muffin-tin-orbital (LMTO) method in the local density and atomic sphere (ASA) approximations according to the Stuttgart code.[31] The radii of the Wigner-Seitz (WS) spheres, which are specifically tabulated in Supporting Information, were assigned automatically so that the overlapping potentials would be the best possible approximations to the full potentials. In general, the WS radii occurred over the following ranges: Na, 1.91–2.24 Å; Au, 1.54–2.24 Å; and Ga, 1.46–1.57 Å. I and II needed no interstitial spheres to achieve space filling in the ASA with an 18% overlap limit between atom-centered spheres,, but III and IV required one each. The basis sets were 3*s*/(3*p*) for Na, 5*d*/(5*f*)/6*s*/6*p* for Au, and 4*s*/4*p*/(4*d*) for Ga, with orbitals in parentheses downfolded.[32] Scalar relativistic effects were included in the calculations. Integrated quantities and density of states (DOS) curves were evaluated using 95, 105, 72, 80 *k*-points in the irreducible wedges of the corresponding Brillouin zones for I–IV, respectively. For bonding analyses, crystal orbital Hamilton population (COHP) curves and their integrated (ICOHP) values were evaluated over occupied states.[33]

RESULTS AND DISCUSSION

Continued systematic exploration of the Na–Au–Ga system in the Na-poor regions (less than 33.3 at. % Na) have yield four new interesting representatives, all of which crystallize with complex polyanionic (Au, Ga) and/or polycationic (Na) networks that exhibit novel building blocks. The four phases, $Na_{1.00(3)}Au_{0.18}Ga_{1.82(1)}$ (I), $NaAu_2Ga_4$ (II), $Na_5Au_{10}Ga_{16}$ (III), and $NaAu_4Ga_2$ (IV) emerge from various locations in this phase space and allow assessments of the influence of different structural chemical factors on their formation, especially for the polyanionic networks. In particular, the Na concentration is found to play a significant role in formation of the anion environment, although with no direct influence on the symmetry. In I and related Na–Au–Ga Bergman-type phases (~32 at. % Na),[16] the anion coordination number is always close to 12, whereas those in II–IV (~15 at. % Na) are mostly 9–11 and, within that range, higher for the anionic component with the higher content. The optimal coordination numbers of Na in Au and Ga systems would be 15–17 according to their relative sizes; however, Na in contrast to all other alkali metals prefers to form fused clusters. Each Na atom in such clusters does not exactly center its own polyhedron but moves closer to other Na atoms and the common cluster center, so such "clusters" can be called multicentered clusters. Such clusters containing Na pairs or triangles are observed in I, III, and IV, whereas those in II are better classified as independent with shared faces.

Crystal Structures. $Na_{1.00(3)}Au_{0.18}Ga_{1.82(1)}$ (I), which crystallizes in a hexagonal crystal class with the refined unit cell formulation $Na_{30.1(7)}Au_{5.4}Ga_{54.6(1)}$, is part of a limited group of compounds with similar structural motifs that have different Pearson symbols in the range of *hP*90–93, and cannot be assigned formally to a single structure type. Other examples include $Na_8K_{23}In_{48}Cd_{12}$,[34] two compositions within the series $Na_{30.5}Ag_xGa_{60-x}$,[35] and the recently reported $BaIn_{1.12}Li_{0.98}$.[26] As was shown for the Ag homologues,[35] the crystal structure of I

dx.doi.org/10.1021/ic401580y | Inorg. Chem. 2013, 52, 12502–12510

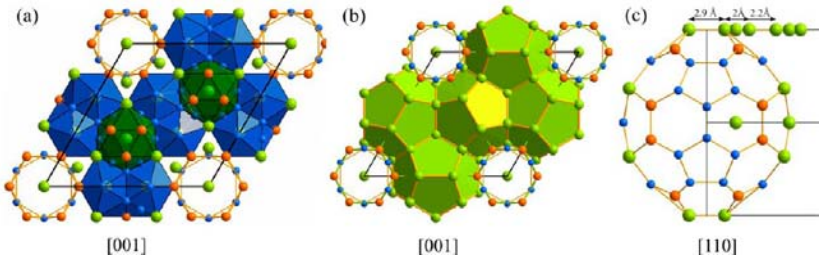

Figure 1. Crystal structure of **I** ($NaAu_{0.2}Ga_{1.8}$): (a) $Na_8(AuGa)_{14}$ (blue) and $Na_6(AuGa)_{18}$(green) polyhedra centered by Na pairs, (b) Clathrate-like network of Na_{20} pentagonal dodecahedra (light green), and (c) Bergman-type cluster. Na, Au, and Ga atoms are green, orange, and blue, respectively.

(see Figure 1) can be described as an hierarchical relative of the $CaCu_5$-type[36] on replacing polyhedra with atoms. In **I**, M_3 (M = Au, Ga) triangles occupy twofold Cu1 positions, Na@M_{18} hexagonal prismatic clusters sit at the Ca positions, and empty M_{12} icosahedra lie in remaining threefold Cu2 sites. Although this structural relationship is useful to understand general aspects of the crystal structure, it fails to include all cation positions so that their structural-chemical roles remain unclear. In ~$NaAu_3Ga_2$, which is precisely formulated as $Na_{13}Au_{41.2}Ga_{30.3}$,[3] Na atoms were observed in multicentered clusters built of two or three symmetric parts with common faces. These centering Na atoms were always slightly shifted toward the common center.[3] A similar situation is also observed in **I**. The structure can be divided into groups of bicentered clusters parallel to the *c*-axis (green) and situated in the *a*-*b* plane (blue) (Figure 1a). The situation along 00*z* is quite different owing to the larger tunnels with disordered Na positions. In this case, the clusters are best described as six penetrating flower leaves around a central stem. Na pairs, centering all clusters, are always separated by Au/Ga hexagons in analogy with ~$NaAu_3Ga_2$. Of course, in all of the above examples Na is also included in cluster shells following its rather high concentration in the compound. The observed cluster packing leaves two kinds of voids: the above-mentioned M_{12} icosahedra and M_{18} capped hexagonal prisms centering, respectively, unit cell edges and the *c*-axis.

To date, Na atoms in the Na−Au−Ga system exhibit enhanced covalency among structures containing ~33 at. % Na.[16] All compounds with compositions between Na_7Ga_{13} and $Na_{26}Au_{36}Ga_{19}$ contain penetrating polyanionic (Au/Ga) and polycationic (Na) nets, and almost all of them contain clusters with local icosahedral symmetry. Since **I** is situated among cubic $Na_{26}Au_{18}Ga_{36}$ and two rhombohedral Bergman-like phases Na_7Ga_{13}[21] and $Na_{17}Au_{5.9}Ga_{46.6}$,[20] Bergman-type building blocks are anticipated. The Ga-based icosahedra in **I** are also surrounded by Na_{20} pentagonal dodecahedra and larger M_{12} icosahedra, like cubic $Na_{26}Au_{18}Ga_{36}$. The dodecahedra form a polycationic Na network via face- and edge-sharing reminiscent of structural motifs in clathrate-type structures with three small cages (Figure 1b, green) and one large cage per cell. The latter polyhedron (Na_{30}, Figure S5) contains two hexagonal, twelve pentagonal, and six rhombic faces along 00*z*. The fourth shell, a buckyball-like 60-atom polyhedron, is slightly different from the typical Bergman-type cubic representatives and includes twelve Na atoms (Figure 1c). Such inclusions, which have not been observed in either the cubic or rhombohedral modifications, lead to visible distortions of the 60-atom polyhedron. However, the main distortion comes from the disordered axial Na positions. $(Na/Au/Ga)_{60}$ clusters stack together in the *ab*-plane and interpenetrate along *c*, resulting in two clusters per unit cell.

Tunnels with highly disordered cations are not a new event in the Na−Au−Ga system. In $Na_{0.56}Au_2Ga_2$[3] uniform tunnels formed of parallel eight-membered rings yield strong disorder of the Na positions along the *c*-axis. The optimal cation positions between two anionic layers were estimated according to difference Fourier maps and electronic structure calculations. A somewhat different situation occurs in **I** as the tunnels along the *c*-axis are formed by alternating anionic and cationic rings. Three anionic layers separated by a Na_6 ring lead to some changes in cation localization in the tunnels. Three Na positions with a total occupancy very close to two atoms per cell and short interatomic distances of ~1 Å were estimated, giving just a mathematical hint of disorder. In contrast to the situation in $Na_{0.56}Au_2Ga_2$,[3] these Na positions in **I** are surrounded by mixed Au/Ga hexagons with maximal possible distances to neighboring Na_6 layers. On the other hand, electron density Fourier maps calculated on the same basis provide much more useful information about the nature of the disorder. Figure 2 shows the distribution of the electron density

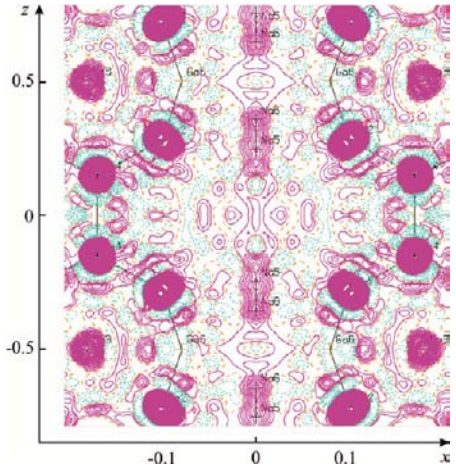

Figure 2. Electron density sections though the vertical *c* axes in$NaAu_{0.2}Ga_{1.8}$. The contour level is 1.0 $e^-/Å^3$, with blue lines for negative values.

in the *x*0*z* plane. In this section, not all neighboring atoms are visible; however, the largest electron density peak in the tunnel (Na_5) is clearly surrounded by heavy atom positions (Au/Ga_2) and there is almost no electron density at $z = 0$ (surrounded by Na_6) and at $z = 1/2$ (surrounded by Ga_6). Na5−Na5 distances are quite large in both directions along the *c*-axis, 4.305 Å within the cell and 4.824 Å between cells, allowing large

dx.doi.org/10.1021/ic401580y | Inorg. Chem. 2013, 52, 12502−12510

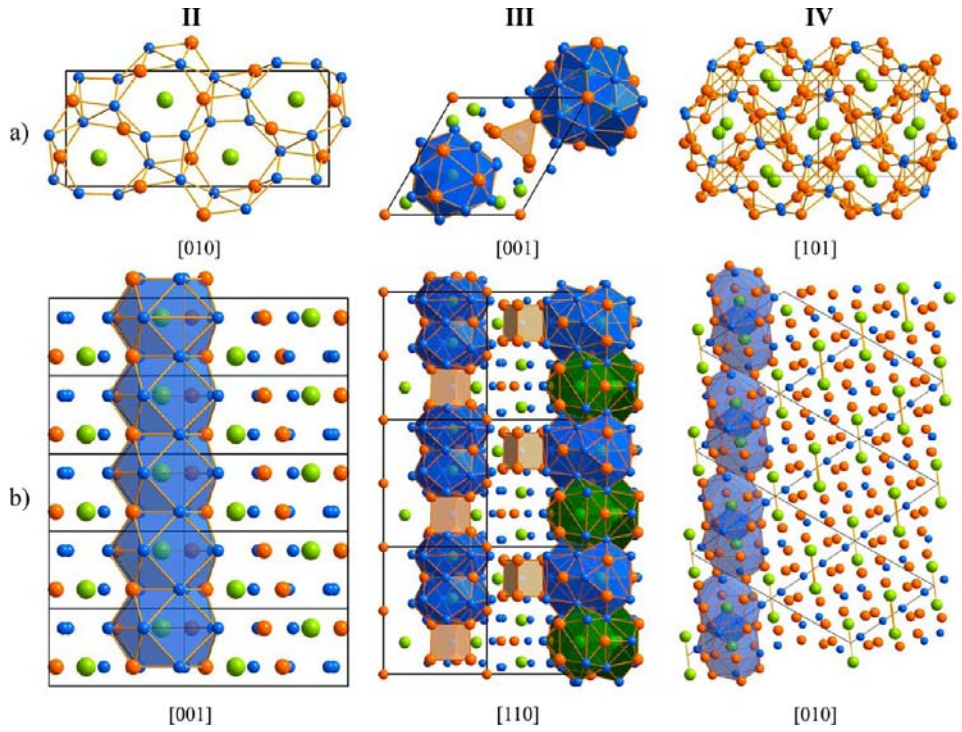

Figure 3. Crystal structure of **II** ($NaAu_2Ga_4$), **III** ($Na_5Au_{10}Ga_{16}$), and **IV** ($NaAu_4Ga_2$). Projections are along the tunnels in (a) and orthogonal to them in (b). Na-centered polyhedra are marked blue and green and Ga-centered Au_6 prisms brown. Au, Ga, and Na atoms are orange, blue, and green, respectively.

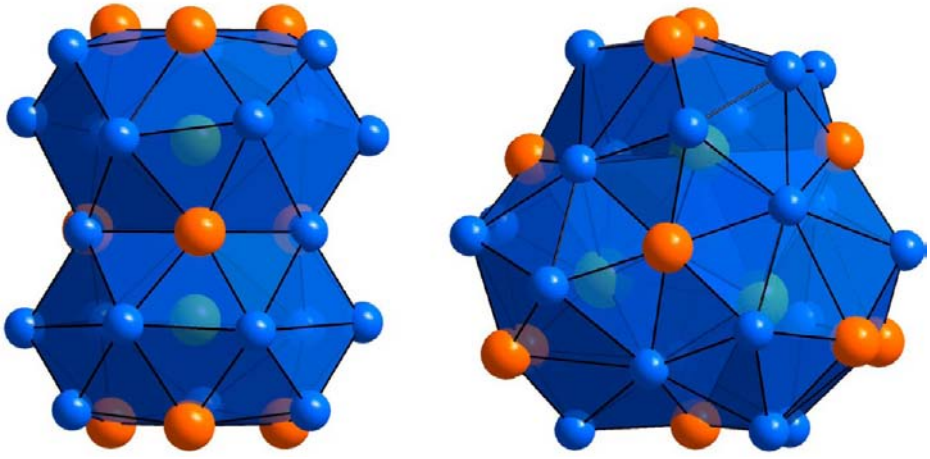

Figure 4. $Na_2@Au_9Ga_{21}$ and $Na_3@Au_{11}Ga_{21}$ polyhedra in the crystal structure of **III** ($Na_5Au_{10}Ga_{16}$).

degrees of freedom. This large volume of unoccupied space may result in a redistribution of the electron density (positions Na6 and Na7, Figure 1c) to allow more reasonable interatomic distances. Another reason for the distance change could be the Bergman-type cluster, fourth shell of which is slightly elongated (Figure 1c) because of the disordered Na positions. The Na5 *z*-coordinate is slightly off the ideal position required for this polyhedron, so some shift toward the origin (position Na7) is expected and limited only by the size of Na. From another viewpoint, these shifts increase the free space between the Na atoms which may be compensated by Na6.

$NaAu_2Ga_4$ (**II**), the isoproportional representative of the heavier analogue KAu_2Ga_4,[2] crystallizes orthorhombic, but in a lower symmetry space group, *Pnma* rather than *Immm*. Its crystal structure is best described as Au/Ga tunnels with encapsulated Na cations. At first look, $NaAu_2Ga_4$ appears to be similar to the structure type of $LaCu_6$,[37] which has the same Pearson symbol *oP*28. However, the unit cell volumes and parameter ratios are quite different and **II** crystallizes in its own structure type. The main building units in **II** are Na-centered, fivefold-capped hexagonal prisms $Na@Au_5Ga_{12}$, the packing of which (Figure 3a) leaves distorted pentagonal prismatic voids. These units stack along the *b*-axis sharing Au_2Ga_4 hexagons and share AuGa edges with eight others to form a zigzag arrangement of $Na@Au_5Ga_{12}$ cages. The smaller size of Na compared with K promotes a lower coordination number (CN_{Na} = 17), and the surrounding polyhedra are not as symmetric as in KAu_2Ga_4 (CN_K = 20). Rather, they resemble those in KAu_3Ga_2, which has a ∼30% lower anion/cation ratio and more efficient atomic packing than in KAu_2Ga_4. Au−Ga

dx.doi.org/10.1021/ic401580y | *Inorg. Chem.* 2013, 52, 12502−12510

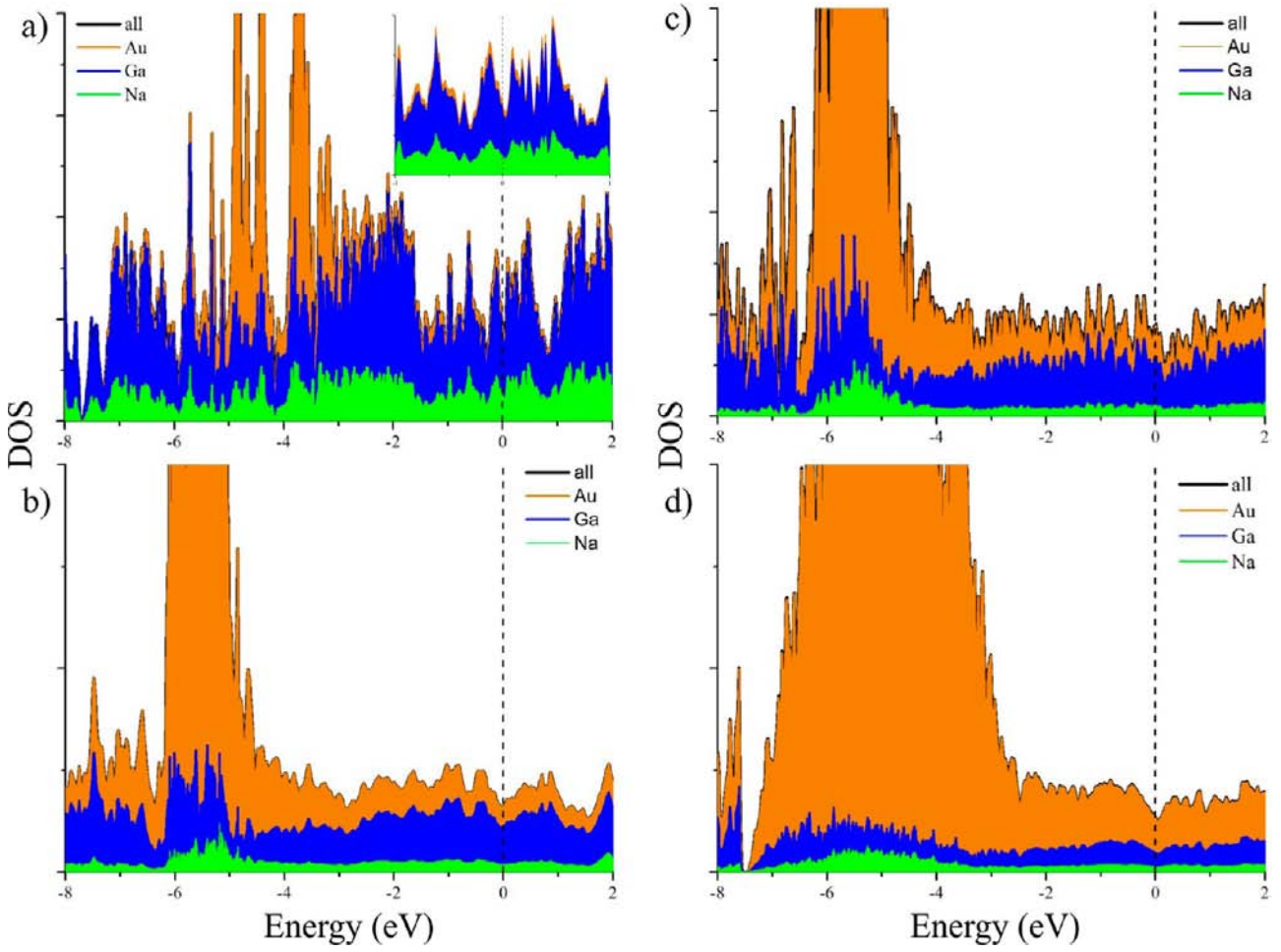

Figure 5. Results of LMTO-ASA calculations for **I**–**IV** (a–d, respectively). (E_F dotted black line). Density of states: (DOS) total DOS (black) and partial DOS curves for gold (orange), gallium (blue), and sodium (green).

and Ga–Ga distances in **II** are in the ranges 2.612(7)–2.757(7) Å and 2.531(7)–2.821(7) Å, which are on average very close to those observed in KAu_2Ga_4, 2.65–2.66 Å and 2.55–2.92 Å, respectively. No close Au–Au contacts are found in **II**. Na–Au and Na–Ga distances are relatively large compared with **III**, **IV**, or Bergman-type approximants,[16] 3.19(2)–3.27(2) Å and 3.19(2)–3.46(3) Å, respectively.

$Na_5Au_{10}Ga_{16}$ (**III**), together with **I** and ~$NaAu_3Ga_2$,[3] belongs to a family with multicentered polyhedra, which are now partially isolated (Figure 3b). **III** crystallizes hexagonally in a new structure type that is best described on the basis of three different polyhedra: (i) Na_2@Au_9Ga_{21}; (ii) Na_3@$Au_{11}Ga_{21}$; and (iii) centered trigonal prisms Ga@Au_6 (Figure 4). **III**, which is reformulated as $NaAu_2Ga_{3.2}$, has a number of similarities to ~$NaAu_3Ga_2$,[3] including symmetry, bi- and tricentered polyhedra, and polyanionic clusters, while adopting a composition close to an inverse Au/Ga content. Since two similar structures with nearly inverse Au/Ga content and fixed Na proportions are already known in the Na–Au–Ga system, i.e., Bergman-type $Na_{13}Au_9Ga_{18}$ and stuffed $Na_{13}Au_{18}Ga_{9.5}$,[16] then similar structures for $NaAu_2Ga_{3.2}$ and ~$NaAu_3Ga_2$ would not be surprising. Albeit similar, the basic polyhedra in **III** differ from those in ~$NaAu_3Ga_2$ mainly in coordination numbers and connection type within the tunnel. In particular, those in **III** are segregated into separate parts and do not build continuous channels as in ~$NaAu_3Ga_2$.

Na_2@Au_9Ga_{21} consists of two face-sharing Na@Au_6Ga_{12} units; however, a cation shift of ~10% toward the common center does not allow their description as independent building blocks. These Na_2-centered polyhedra can also be described using parallel *n*-membered Au/Ga rings. ~$NaAu_3Ga_2$ contains two different units, 4–6–6–6–4 and 7–6–6–6–7, whereas **III** only has (3 + 3)–6–6–6–(3 + 3) (Figure 4a), which consist of three hexagons and two triangles capped by additional triangles in ways that have not been recognized in any related compound.[3] Tricentered polyhedra in $NaAu_2Ga_{3.2}$ and ~$NaAu_3Ga_2$ are also slightly different: Na atoms in **III** belong to the coordination sphere of each other (Figure 4b), while those in ~$NaAu_3Ga_2$ are well separated. The coordination number of Na in the Na_3@$Au_{11}Ga_{21}$ is 17 including two neighboring Na atoms at distances of 3.318 Å. Three Na@$Na_2Au_6Ga_9$ units share hexagonal $NaAu_3Ga_2$ faces in the *ab*-plane and Au_2Ga triangles along the *c*-axis. Na_3 triangles centering each polyhedron are rotated by 60° around the *c*-axis toward each other, resulting in no voids along this direction, similar to ~$NaAu_3Ga_2$. The Ga@Au_6 prisms in **III** (Figure 3, brown) appear as bridges between Na_2@Au_9Ga_{21} along the *c*-axis by sharing Au_3 faces. Ga in these prisms has no contacts with Na atoms, which exemplifies a rare case of such anion isolation. Moreover, these prisms are slightly compressed, with Au–Au distances definitely larger than the sum of the covalent radii,[38] 3.232(1) and 3.598(1) Å, and a Au–Ga bond, 2.632(1)

dx.doi.org/10.1021/ic401580y | *Inorg. Chem.* 2013, 52, 12502–12510

Å that is comparable with those in the other Au−Ga compounds.[2] On the other hand, **III** contains a large number (42% in the entire structure) of notably short Na−Au distances, including the shortest Na−Au contact to date of 2.957(8) Å. The Na−Au distances in **III** are comparable to those in $Na_{32}Au_{40}Ga_{28}$[20] and $Na_{0.97}Au_2Zn_4$[17] (within ∼2%) and in Na−Au−Ga Bergman-type compounds[16] (within 3%).

$NaAu_4Ga_2$ (**IV**) is the third compound that has a mirrored composition representative (**II**). **IV** crystallizes in a monoclinic crystal class, and is only the second representative of this class within the A−Au−Tr family (A = alkali metal; Tr = triel element Ga, In, Tl) after K_4Au_8Ga.[39] It is not entirely clear what is responsible for such symmetry lowering in comparison with $NaAu_2Ga_4$ or KAu_2Ga_4; however, both compounds have large Au contents (>50 at. %). **IV** can be conventionally classified as a tunnel structure with a novel, edge-sharing type connection between the Na-centered (Au, Ga) chains, in contrast to $A_{0.55}Au_2Ga_2$ and AAu_3Ga_2[3] with large shared faces or even polyhedra. In terms of the population of the parallel 4−6−6−6−4 membered rings, the $Na_2@Au_{18}Ga_8$ examples in **IV** are very close to those in ∼$NaAu_3Ga_2$. Na−Na distances within these units are 3.627(2) Å, which is ∼10% greater than those in **III**, whereas Au−Au and Au−Na distances are quite short, with the lower limit, respectively, of 2.753(1) and 2.968(4) Å. The latter is within the 3σ range of 2.957(8) Å in **III**.

The zigzag chains formed by separate Na pairs in **IV** ($NaAu_4Ga_2$, Figure 3) are very different from those in AAu_3Ga_2 (A = K, Rb, Cs)[2,3] with almost doubled interpolyhedral Na−Na distances in comparison with those along a chain; whereas all A−A contacts in AAu_3Ga_2 are interpolyhedral and identical. The relative orientation of zigzag chains in **IV** allows us to compare its features with $RbAu_3Ga_2$ and $CsAu_3Ga_2$:[3] A_2 pairs in two neighboring tunnels lie in nearly perpendicular planes, whereas those in KAu_3Ga_2[2] are parallel with each other. Another analogy is evident from comparison with the temperature-dependent modifications of $LaCu_6$,[37,40] which crystallize with the same orthorhombic (high-*T*) and monoclinic (low-*T*) space groups as **II** and **IV**. Although **II** and **IV** retain similar structural motifs to $LaCu_6$, they adopt their own structure types. The diversity comes mainly from different cation sizes and coordination numbers, which have direct influence on the surrounding anionic network. In these cases, the relative cation sizes and contents of the anionic components (Au and Ga) appear to exert the greatest influences on the type of polyanionic networks formed.

Electronic Structure and Chemical Bonding. DOS curves were calculated for a slightly idealized model "$Na_{30}Au_6Ga_{54}$"of **I** and the hypothetical model "$Na_{30}Ga_{60}$" to check the influence of Au on the electronic structure. Two Au/Ga mixed positions were assigned as pure Au (6*m* site 1) and Ga (12*n* site 2), resulting in a composition that is very close to that obtained from the X-ray structure analysis. All Na peaks along 00*z* have been combined into two fully occupied 001/4 and 003/4 sites. The DOS curves for **I** exhibit broad valence Na and Ga *s* and *p* bands and a large but narrow Au 5*d* band that is located 3−5 eV below E_F (Figure 5a), a feature that corresponds with the low Au content and questions the importance of Au toward formation of this compound. The Fermi level in **I** is situated in a narrow but very sharp pseudogap that also intersects a high DOS region, indicative of metallic behavior. The minimum of the pseudogap occurs for 198.7 valence electrons per cell, which is within 3σ of 199.2 valence electrons obtained from single crystal X-ray refinements (the model "$Na_{30}Au_6Ga_{54}$" has 198 valence electrons). There is also a slightly deeper pseudogap at +0.8 eV, which corresponds to 218 valence electrons, and suggests a possibility of partial substitution of Na by divalent cations. On the other hand, the DOS curve of the hypothetical model "$Na_{30}Ga_{60}$" (Figure S6) reveals a pseudogap at 0.35 eV below the Fermi level, that corresponds to 202 valence electrons and is again very close to the experimentally observed value of 199.2. This last outcome allows a "rigid-band" approach and suggests that Au serve primarily as an electronic oxidizing agent., appropriate to its large absolute electronegativity.

The narrow pseudogap in the DOS curve of **I** might explain the absence of an observed homogeneity range in spite of mixed Au/Ga positions and cation disorder. The latter also raises questions about any participation of Na in covalent interactions. Theoretical simulations and analyses of Fourier maps for $A_{0.55}Au_2Ga_2$ (A = Na, K, Rb, Cs)[2] indicate that the most appropriate cation position in a polyanionic tunnel is between the two neighboring rings within octagonal antiprisms, whereas a second site, surrounded by only one ring, is metastable. Stable cases of cation displacements exist too; however, these lead to deformed tunnels and stacked cages as in KAu_3Ga_2 or KAu_2Ga_4. An unusual situation is observed in **I** with nearly uniform tunnels containing one special feature − a cationic layer between each group of three anionic layers, so the tunnel can be described as $(Na_6(Au/Ga)_6Ga_6(Au/Ga)_6)_n$. According to COHP analysis, the populations of Na−Ga(Au) bonds within and around the tunnel average 0.18 eV/bond and are extremely large compared with those in the center of the unit cell. The largest populations, 0.30−0.32 eV/bond, have been found within Na and Ga/Au hexagons forming the tunnel walls and for Na−Ga bonds formed by central Ga_6 hexagon and two Na hexagons surrounding the tunnel. The latter can be explained as an electronic compensation for the partial separation of Na and Ga within the tunnel. The ICOHP values for the contacts between the disordered Na positions and tunnel walls are also large, ∼25% above the average value. The last two facts may explain why the cation disorder in **I** is not as large as in $A_{0.55}Au_2Ga_2$ phases. It is not unusual that Ga(Au)−Ga(Au) bonds provide the greatest contribution to the total orbital populations, 82.6%; however, Na−Ga(Au) interactions contribute 17.4%, which is high and comparable with that in Ga-rich Bergman-type phase and the orthorhombic approximant phase $Na_{32}Au_{40}Ga_{28}$, in spite of its very low Au content.

The DOS curves for $NaAu_2Ga_4$ (**II**), $Na_5Au_{10}Ga_{16}$ (**III**), and $NaAu_4Ga_2$ (**IV**) are qualitatively similar and also show metallic characteristics. They exhibit broad valence *s* and *p* bands and a large, mostly Au 5*d* band located 3−7 eV below E_F depending on Au content in the compound (Figure 5 b,c,d). Analyses of the partial DOS curves show comparable contributions from Au and Ga states to the total DOS in **II** and **III,** and a major contribution of Au in **IV** that is usual for such types of compounds. The role of Na in these compounds can be characterized as a formal one-electron donor, although Na−Au and Na−Ga ICOHP values do not afford a comparison with that of K^+ in KAu_3Ga_2 or $K_{0.55}Au_2Ga_2$.[2] The COHP analysis of **III** showed that it has features similar to **II** and **IV**. Au−Ga together with Ga−Ga in **II** and **III** and Au−Au in **IV** provide more than 90% to the total orbital interactions (Table 4, Figure 6), which is predictable given the low Na contents. More interesting information comes from the COHP analysis of Na−Au and Na−Ga pairs in **II** and **IV**, which are situated on the

Table 4. Bond Length Ranges and Average −ICOHP Values in II−IV

bond type	lengths (Å)	−ICOHP (eV/per aver. bond)	*n*/ cell	−ICOHP (eV/ cell)	contribution (%)
		$NaAu_2Ga_4$(**II**)			
Au−Ga	2.612−2.722	1.73	52	90	72.2
Ga−Ga	2.531	1.04	24	25.0	20.0
Na−Au	3.190−3.281	0.15	20	3.0	2.4
Na−Ga	3.19−3.35	0.12	56	6.7	5.3
		$Na_5Au_{10}Ga_{16}$(**III**)			
Au−Au	3.233	0.42	6	2.5	0.8
Au−Ga	2.571−2.685	1.67	123	204.9	71.2
Ga−Ga	2.686−2.900	1.1	58	63.9	22.2
Na−Au	2.958−3.428	0.16	54	8.71	3.0
Na−Ga	3.144−3.387	0.14	54	7.76	2.7
		$NaAu_4Ga_2$(**IV**)			
Au−Ga	2.559−2.793	1.61	66	106	65.0
Au−Au	2.754−2.973	1.20	38	45.6	27.9
Ga−Ga	2.852	0.51	4	2.0	1.2
Na−Au	2.968−3.243	0.15	44	6.6	4.0
Na−Ga	3.174−3.247	0.12	24	2.9	1.8

same Na concentration line and can be used to characterize the cation-poor region. They have slightly different numbers of Na−M (M = Au and Ga) contacts and the ratios of these contacts to the total number of bonds per unit cell follow their structural differences. Na−M contributions in **II** and **IV** are 7.7 and 5.7%, respectively, of the total ICOHP values. These values are disproportionally lower than those in **I** and in the cubic and orthorhombic approximants close to the Na−Au−Ga QC, all of which occur at the ∼32 at. % Na concentration line and are characterized by higher, up to 18%, contributions of the Na−M pairs. Detailed analyses of these Na−M pairs reveal that ICOHP values for **II** and **IV** are 0.15 and 0.12 eV/bond for Na−Au and Na−Ga, respectively, whereas those for the Na-richer compounds are in the ranges 0.18−0.20 and 0.15−0.17 eV/bond, respectively. Therefore, increasing Na content leads to not only larger contributions to the total ICOHP, but also to the partial redistribution of the electronic population within the structure and larger involvement of the cations in covalency.

These results differ significantly from those of the K−Au−Ga compounds with similar cation proportions, which show almost negligible contributions from K−Au(Ga) pairs.[2] Moreover, heteroatomic Au−Ga bonds are always dominant over Au−Au and Ga−Ga bonds in **II** and **IV**. They present ∼35% of the total number of bonds and provide the greatest contribution to the total orbital interactions, 60−70%. As seen in the COHP curves in Figure 5, Na−Au, Na−Ga, Au−Au, and Ga−Ga orbital interactions in **II** and **IV** are nearly optimized at E_F, and a larger number of valence electrons would populate Ga−Ga antibonding states, whereas Au−Ga interactions remain bonding above E_F. The last indicates the dominant role of polar bonding interactions in the stability of such phases.

The similar structural building principles among **II**, **III**, and **IV** certainly contribute to their similarities in electronic structure. **III** and **IV** have evident but moderate pseudogaps in the vicinity of the Fermi levels; in **II**, E_F falls near a local minimum. The pseudogap for **III** occurs distinctly at 128 valence electrons per unit cell ("$Na_5Au_{9.5}Ga_{16.5}$"), very close to the refined count of 126 ($Na_5Au_{10}Ga_{16}$). In this case, some possibility of mixed occupations of the anion (Au/Ga) positions cannot be excluded, although such a condition is very rare in other cation-poor compounds among related systems. For example, the homogeneity ranges in KAu_3Ga_2 and $\sim NaAu_3Ga_2$ are very limited (1−2%). On the other hand, geometrical and bonding characteristics of Na might explain why no other representatives of these structure types have been discovered. **II** and **IV** have several isoproportional (AX_2Y_4) relatives with many different electropositive (A) and electronegative (X, Y) atoms possible,[2,37,40−42] but even those with the same Pearson numbers crystallize with more or less different structures. A representative case, which was mentioned above, appears to be $LaCu_6$, which has both orthorhombic and monoclinic modifications and even the same space groups as $NaAu_2Ga_4$ (**II**) and $NaAu_4Ga_2$ (**IV**), but not identical structures in either case. Although the valence electron-to-atom ratios for $LaCu_6$ and **IV** are identical, 2.14 (excluding valence *d*-electrons for Cu and Au), the cation sizes and cation/anion size ratios reveal the greater influence of the polyhedron types and their packing, leading to the difference between both modification of $LaCu_6$ and $NaAu_2Ga_4$ or $NaAu_4Ga_2$.

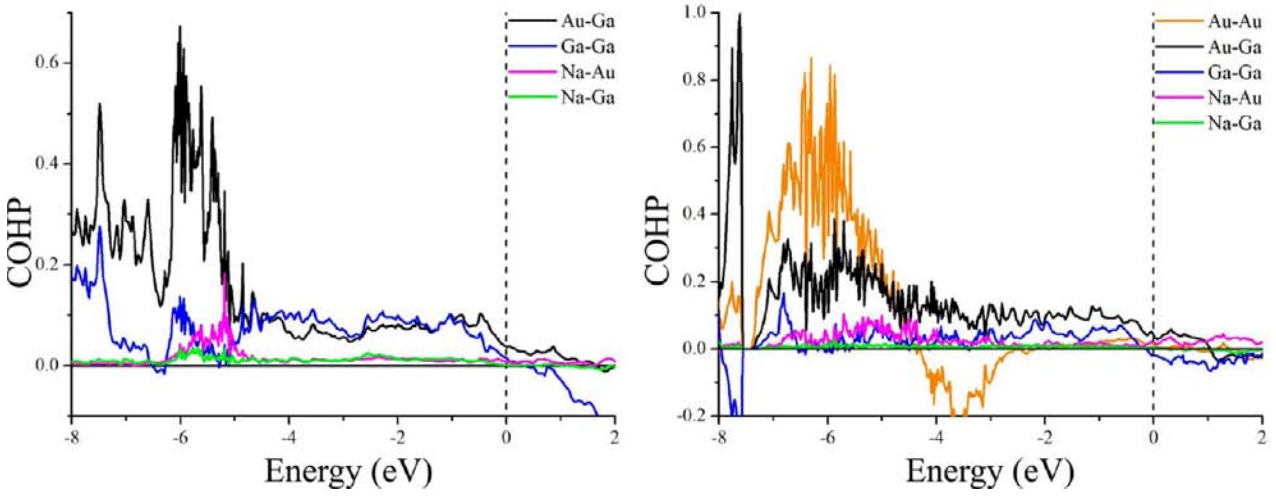

Figure 6. COHP data for five interactions in **II** and **IV** (left and right) (E_F dotted black line): Au−Ga (black), Au−Au (orange), Ga−Ga (blue), Na−Au (magenta), and Na−Ga (green).

dx.doi.org/10.1021/ic401580y | *Inorg. Chem.* 2013, 52, 12502−12510

SUMMARY

Herein, we have presented the syntheses and structures of four new Na−Au−Ga compounds that exhibit very complex 3-D networks. Within the group, $Na_{1.00(3)}Au_{0.18}Ga_{1.82(1)}$ (**I**) represents the Na-rich line, elements of local fivefold symmetry, and a clathrate-like polycationic network. On the other hand, elements of tunnel structures and multicentered polyhedra have been also observed in this collection. Thus, **I** appears to be a unique compound containing structural features that are observed in the both ∼15 atom % and ∼32 atom % Na-concentration-dependent groups. $NaAu_2Ga_4$ (**II**), $Na_5Au_{10}Ga_{16}$ (**III**), and $NaAu_4Ga_2$ (**IV**) are representatives of the Na-poor group and yield three new structure types. Since they show clear differentiations from both **I** and Na-rich quasicrystal approximants, influence of both geometrical and electronic factors on the formation of new compounds was investigated. Na atoms in **I**, **III**, and **IV** show no ability to form isolated clusters and always condense into bi- or tricentered conglomerates with large common faces, which are as a rule hexagonal. Na atoms do not exactly center each polyhedron but are shifted toward the center of the clusters formed by two or three condensed polyhedra. A somewhat different situation is found in **II** in which centered polyhedra form tunnels similar to those in the isoproportional K analogue.

Electronic structure calculations showed that all compounds are metallic in nature with evident pseudogaps at the Fermi levels, except in **II**. The overall bond populations are dominated by polar Au−Ga bonds, typical for such compounds. The major involvement of Na into covalent bonding interactions observed in **I** follows the behaviors observed for the ∼32 at. % concentration line in the same system.[7,16] On the other hand, contributions of Na in **II**, **III**, and **IV** suggest that such involvements depend also on atom proportions in the compound and increase disproportionally with Na concentration.

ASSOCIATED CONTENT

Supporting Information

Measured and simulated powder X-ray diffraction patterns of **I**, **III**, **IV**; section of Na-Au-Ga phase diagram around 350 °C; Na_{30} cage identified in **I**; electronic DOS curve of "$Na_{30}Ga_{60}$" to mimic **I**; and table of Wigner-Seitz radii used in TB-LMTO-ASA calculations. This material is available free of charge via the Internet at http://pubs.acs.org.

AUTHOR INFORMATION

Corresponding Author

*E-mail: gmiller@iastate.edu.

Notes

The authors declare no competing financial interest.

ACKNOWLEDGMENTS

The research was supported by the Office of the Basic Energy Sciences, Materials Sciences Division, U. S. Department of Energy (DOE). Ames Laboratory is operated for DOE by Iowa State University under contract No. DE-AC02-07CH11358.

REFERENCES

(1) Corbett, J. D. *Inorg. Chem.* **2010**, *49*, 13.
(2) Smetana, V.; Corbett, J. D.; Miller, G. J. *Inorg. Chem.* **2012**, *51*, 1695.
(3) Smetana, V.; Miller, G. J.; Corbett, J. D. *Inorg. Chem.* **2012**, *51*, 7711.
(4) Li, B.; Kim, S.-J.; Miller, G. J.; Corbett, J. D. *Inorg. Chem.* **2009**, *48*, 6573.
(5) Lin, Q.; Corbett, J. D. *Inorg. Chem.* **2011**, *50*, 1808.
(6) Lin, Q.; Corbett, J. D. *Inorg. Chem.* **2007**, *46*, 8722.
(7) Smetana, V.; Lin, Q.; Pratt, D.; Kreyssig, A.; Ramazanoglu, M.; Corbett, J. D.; Goldman, A.; Miller, G. J. *Angew. Chem., Int. Ed.* **2012**, *51*, 12699.
(8) Li, B.; Corbett, J. D. *Inorg. Chem.* **2007**, *46*, 6022.
(9) Herbstein, F.; Marsh, R. *Acta Crystallogr. B* **1983**, *39*, 280.
(10) van Vucht, J. *J. Less-Common Met.* **1985**, *108*, 163.
(11) Bergman, G.; Waugh, J. L. T.; Pauling, L. *Acta Crystallogr.* **1957**, *10*, 254.
(12) Lee, C. S.; Miller, G. J. *J. Am. Chem. Soc.* **2000**, *122*, 4937.
(13) Doering, W.; Schuster, H. U. *Z Naturforsch. B* **1979**, *34*, 1757.
(14) Lee, C. S.; Miller, G. J. *Inorg. Chem.* **2000**, *40*, 338.
(15) Tillard-Charbonnel, M.; Belin, C. *J. Solid State Chem.* **1991**, *90*, 270.
(16) Lin, Q.; Smetana, V.; Miller, G. J.; Corbett, J. D. *Inorg. Chem.* **2012**, *51*, 8882.
(17) Samal, S. L.; Lin, Q.; Corbett, J. D. *Inorg. Chem.* **2012**, *51*, 9395.
(18) Corbett, J. D. In *Chemistry, Structure and Bonding of Zintl Phases and Ions*; Kauzlarich, S., Ed.; VCH Publishers: New York, 1996.
(19) Miller, G. J.; Schmidt, M.; Wang, F.; You, T.-S. *Struct. Bonding (Berlin)* **2011**, *990*, 1.
(20) Smetana, V.; Corbett, J. D.; Miller, G. J. *J. Solid State Chem.* **2013**, *207*, 21.
(21) Frank-Cordier, U.; Cordier, G.; Schaefer, H. *Z .Naturforsch. B* **1982**, *37*, 119.
(22) Sevov, S. C.; Corbett, J. D. *Inorg. Chem.* **1992**, *3*, 1895.
(23) Sevov, S. C.; Corbett, J. D. *J. Solid State Chem.* **1993**, *103*, 114.
(24) Pyykkö, P. *Chem. Rev.* **1988**, *88*, 563.
(25) Haucke, W. *Naturwissenschaften* **1937**, *25*, 61.
(26) Smetana, V.; Vajenine, G.; Kienle, L.; Duppel, V.; Simon, A. *J. Solid State Chem.* **2010**, *183*, 1767.
(27) Stoe & Cie GmbH: Darmstadt, Germany, 2004.
(28) Bruker AXS, Inc.: Madison, WI, 1996.
(29) Blessing, R. *Acta Crystallogr.* **1995**, *A51*, 33.
(30) Sheldrick, G. M. University of Göttingen, Göttingen, Germany, 1997.
(31) Tank, R.; Jepsen, O.; Burkhardt, A.; Andersen, O. K. Max-Planck-Institut für Festkörperforschung, Stuttgart, Germany, 1994.
(32) Andersen, O. K.; Jepsen, O.; Gloetzel, D. In Canonical Description of the Band Structures of Metals; *Proceedings of the International School of Physics, "Enrico Fermi"*; Course LXXXIX, Varenna; Bassani, F., Fumi, F., Tosi, M. P., Eds.; North-Holland, Amsterdam, 1985; p 59.
(33) Dronskowski, R.; Blöchl, P. E. *J. Phys. Chem.* **1993**, *97*, 8617.
(34) Flot, D. M.; Tillard-Charbonnel, M.; Belin, C. *J. Am. Chem. Soc.* **1996**, *118*, 5229.
(35) Henning, R. W.; Corbett, J. D.; Lee, S. *Z. Anorg. Allg. Chem.* **2002**, *628*, 2715.
(36) Haucke, W. *Z. Anorg. Allg. Chem.* **1940**, *244*, 17.
(37) Meyer-Liautaud, F.; Allibert, C.; Moreau, J. M. *J. Less-Common Met.* **1985**, *110*, 81.
(38) Cordero, B.; Gomez, V.; Platero-Prats, A.; Reves, M.; Echeverria, J.; Cremades, E.; Barragan, F.; Alvarez, S. *Dalton Trans.* **2008**, *2008*, 2832.
(39) Mueller, J.; Zachwieja, U. *Z. Anorg. Allg. Chem.* **2000**, *626*, 1867.
(40) Asano, H.; Umino, M.; Hataoka, Y.; Shimizu, Y.; Onuki, Y.; Komatsubara, T.; Izumi, F. *J. Phys. Soc. Jpn.* **1985**, *54*, 3358.
(41) Bobev, S.; Bauer, E. *Acta Crystallogr. E* **2005**, *61*, i89.
(42) Salvador, J.; Hoang, K.; Maharti, S.; Kanatzidis, M. *Inorg. Chem.* **2007**, *46*, 6933.